OF-1-13

FREQUENCY-DEPENDENT CHARACTERISTICS OF GAP DISCONTINUITIES IN SUSPENDED STRIPLINES FOR MILLIMETER WAVE APPLICATIONS

Aosheng Rong   Sifan Li

Department of Radio Engineering
Nanjing Institute of Technology
Nanjing, P.R.China

ABSTRACT

In this paper, a full-wave analysis of equivalent circuit parameters of gap discontinuities in suspended striplines is investigated rigorously by resonance method and variational technique. A set of charts of the parameters at W- and Ka-band are evaluated. A Ka-band prototype bandpass filter has been designed and realized to demonstrate the feasibility of the present analysis. The mesured results agree well with the theoretical prediction.

INTRODUCTION

Though the suspended stripline has been extensively used in microwave and millimeter wave integrated circuits for a long time, the rigorous analysis of its discontinuities has not been published yet in literature. Only few papers discussing such a problem by quasi-static method gave out some emperical or approximate results.[1] [2]

In this paper, the gap discontinuities in suspended stripline including microstrip are investigated rigorously by resonance method together with variational technique. Full wave analysis is applied and frequency dispersion effects are taken into account. A set of design charts at Ka-band and W-band are evaluated. Using these results a Ka-band prototype bandpass filter has been designed and tested to demonstrate the feasibility of the present analysis. The measured results agree well with the theoretical predictions.

THEORY

Fig.1 shows the configuration of the gap discontinuity in a a suspended stripline and Fig.2 is its equivalent network. Suppose two magnetic wall set at a distance l_1 and l_2 respectively away from the left and right reference plane of the discontinuity so that a closed resonator is formed. Due to symmetry, $l_1 = l_2 = l$, the equivalent circuit parameters can be determined from the following resonance conditions:

$$Y_{11} - Y_{12} = -j\tan(\beta l_o) \quad (1)$$

$$Y_{11} + Y_{12} = -j\tan(\beta l_e) \quad (2)$$

where β is the phase constant of the dominant mode of uniform suspended stripline. l_o and l_e are distances between the magnetic wall and the reference plane when the symmetric plane of the circuit is electric and magnetic wall respectively. Therefore the problem of calculating Y_{11} and Y_{12} becomes a problem of calculating l_o and l_e which are evaluated by varitional technique.

In Fig.3 the resonator contains the suspended stripline discontinuity and is enclosed by a housing with electric and magnetic walls. Let $\overline{E}$ and $\overline{H}$ represent the trial fields inside the resonator, $\overline{J}$ and $\overline{M}$ stand for current density and magnetic current density in all three regions τ_1, τ_2 and τ_3, and $\overline{J}_s$ $\overline{M}_s$ are coresponding currents on each boundary surfaces. Then $\overline{E}$ and $\overline{H}$ satisfy the following variational equation [3] and Maxwell's equations:

$$\nabla \times \overline{H} = j\omega\varepsilon\overline{E} + \overline{J}, \qquad \nabla \times \overline{E} = -j\omega\mu\overline{H} - \overline{M} \quad (3)$$

$$\iiint_{\tau}(\vec{E}\cdot\vec{J}^* + \vec{H}\cdot\vec{M}^*)d\tau + \iint_{S_c}(\vec{E}\cdot\vec{J}_s^* + \vec{H}\cdot\vec{M}_s^*)\,ds = 0 \quad (4)$$

If $\overline{E}$ and $\overline{H}$ are so chosen that in region $\tau_1 \tau_2$ and τ_3 both $\overline{J}$ and $\overline{M}$ are equal to zero then the first term of equation (4) vanishes. The second term depends on various boundary conditions. Since the wall of the resonator is either electric wall or magnetic wall, the surface integration of this part is zero. For the boundary at $y=h_3$ the tangential components of electric fields on each side are continuous. So do magnetic fields. Therefore the boundary at $y=h_3$ has no contribution to the surface integration. The only boundary needing consideration is that at $y= h_3+d$. The tangential components of electric fields are still continuous at $y=h_3+d$. Hence no magnetic current exists on that boundary. While the tangential components of magnetic fields are not continuous on the stripline surface Sw.

$$\overline{H}_t^{(1)} - \overline{H}_t^{(2)} = \begin{cases} -\overline{J}_s, & \text{on Sw} \\ 0, & \text{except Sw} \end{cases} \qquad (5)$$

Therefore the variational equation (4) becomes

$$\iint_{Sw} \overline{E}_t^{(1)} \cdot \overline{J}_s^{*} \, ds = 0 \qquad (6)$$

$\overline{E}_t^{(1)}$ can be expressed in terms of Hertz potential π^h and π^e for TE and TM mode respectively. By applying boundary conditions and after some necessary manipulation the expression of $\overline{E}_t^{(1)}$ as a function of surface current density $\overline{J}_s$ and a set of dimensions of the resonator is derived. Then let $\overline{J}_s$ expanded into an appropriate series of base function $\overline{J}_{s,k}$ as follows

$$\overline{J}_s = \sum C_k \overline{J}_{s,k} \qquad (7)$$

where $$\overline{J}_{s,k} = J_{zk}(x,z)\overline{u}_z + J_{xk}(x,z)\overline{u}_x \qquad (8)$$

and

$$J_{zk}(x,z) = \frac{1}{\sqrt{1-(\frac{2x}{w})^2}} \frac{\sin\beta(h-|z-z_k|)}{\sin(\beta h)}$$

$$z_k=kh, \; |y|<w, \; |z-z_k|<h,$$

$$J_{xk}(x,Z) = \frac{\sin(\frac{2x\pi}{w})}{\sqrt{1-(\frac{2x}{w})^2}} \frac{\sin\beta(h-|z-z_k|)}{\sin(\beta h)}$$

$$z_k= (k-1)h, \; |y|<w, \; |z-z_k|<h.$$

Substituting Eq. (7) and (8) into (6) and applying Rayleigh-Ritz method yield a set of homogeneous equations which can be expressed in terms of the following matrix equation

$$[A]\,[C] = 0 \qquad (9)$$

where $[C] = [C_1 \; C_2 \; C_3 \; \ldots\ldots C_k]^T$

$$[A] = [A_{kl}]_{k\times k}$$

The matrix element A_{kl} is a function of frequency and the dimensions of the resonator. Once frequency and the configuration of the resonator are given the distance l_o and l_e can be obtained from the following equation

$$\det\,[A] = 0$$

Then from Eq. (1) and (2) Y_{11} and Y_{12} are evaluated

RESULTS

A set of equivalent parameters $jB_s = -Y_{12}$ and $jB_p = Y_{11} + Y_{12}$ of the gap discontinuity in suspended stripline are calculated. Fig.4 and 5 show the parameters at W-band. Fig.6 and 7 show the parameters at Ka-band. It is evident that all these curves are frequency-dependent. Fig.8 is a prototype Ka-band bandpass filter designed for demonstration. The measured result shown in Fig.9 is in good agreement with the theoretical prediction.

REFERENCES

[1] C.Nguyen et al. International Jounal of Infrared and Millimeter Waves, 6(1985), 497-509

[2] I.J.Smith. IEEE Trans. on MTT, 19(1971), 424-431

[3] R.F.Harrington. Time-Harmonic Electromagnetic Fields, New York, McGraw-Hill, 1961.

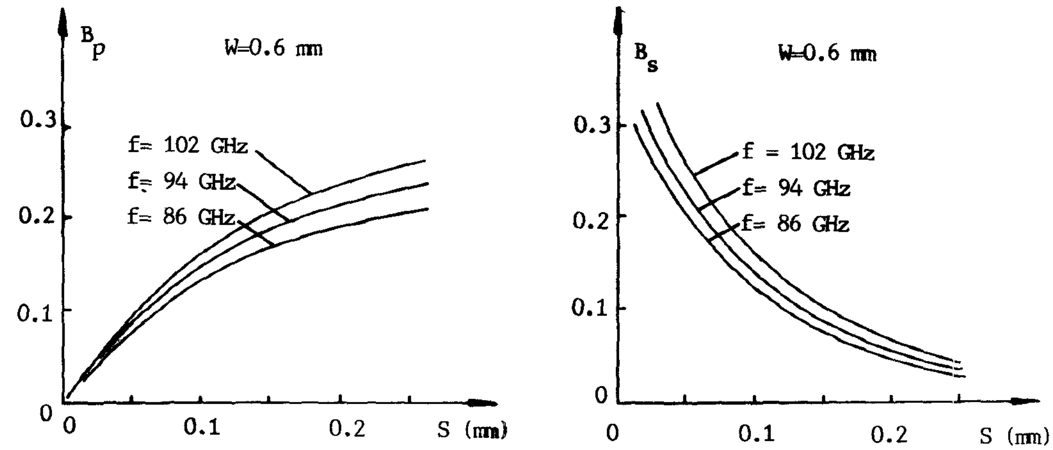

(a) **Fig.4** (b)

a=1.27 mm, b=0.635 mm, h_3=0.318 mm, d=0.127 mm, ε_r=2.22

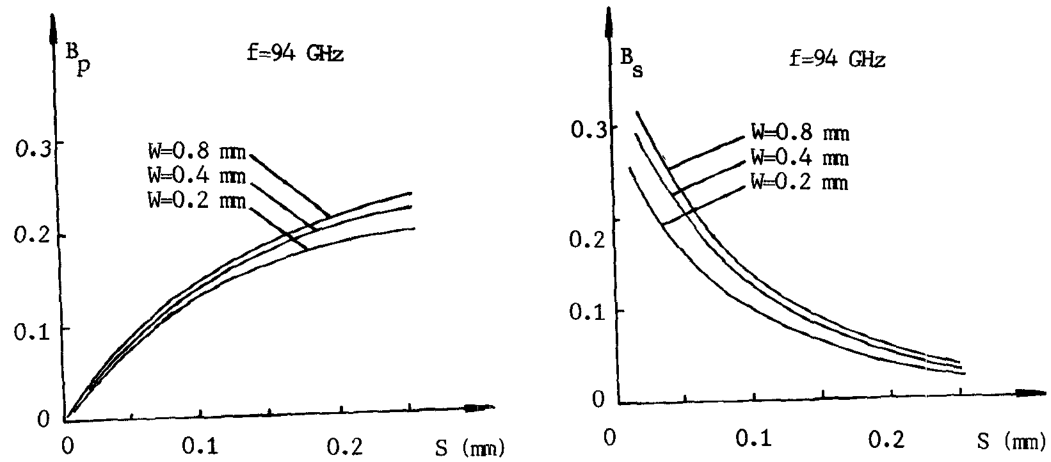

a=1.27 mm, b=0.635 mm, h_3=0.318 mm, d=0.127 mm, ε_r=2.22

(a) (b)

Fig. 5

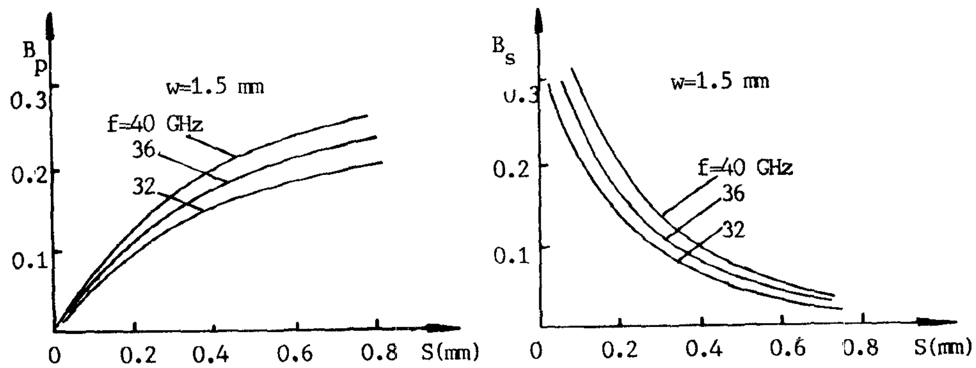

a=3.56 b=1.78 mm h_1=0.89 mm d=0.127 mm ε_r=2.22

Fig. 6

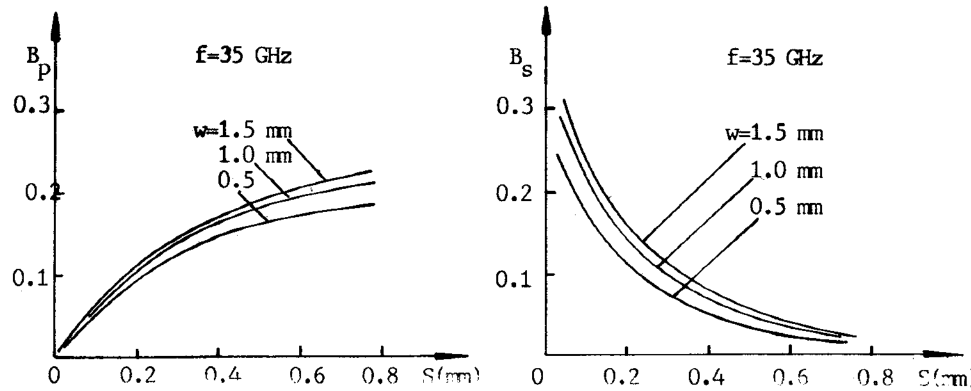

a=3.56 mm b=1.78 mm h_1=0.89 mm d=0.127 mm ε_r=2.22

Fig. 7

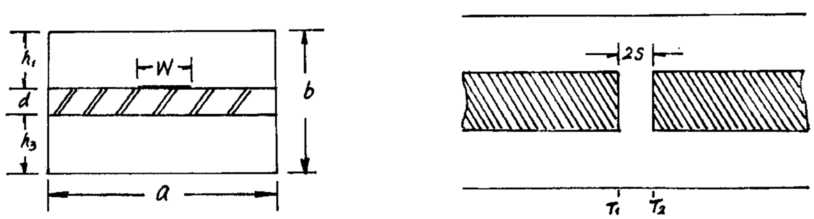

(a) Crosssection

(b) Top view

Fig.1

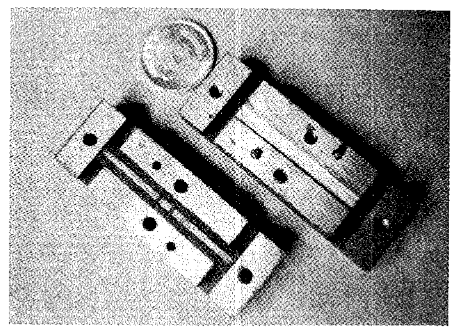

Fig.8

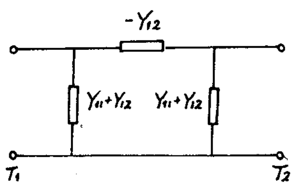

Fig.2

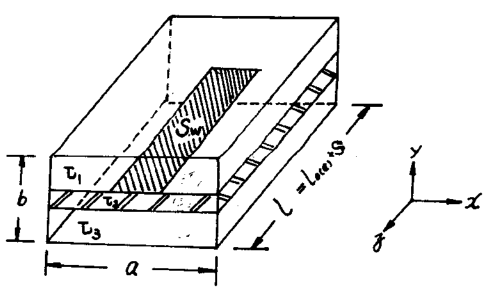

Fig.3

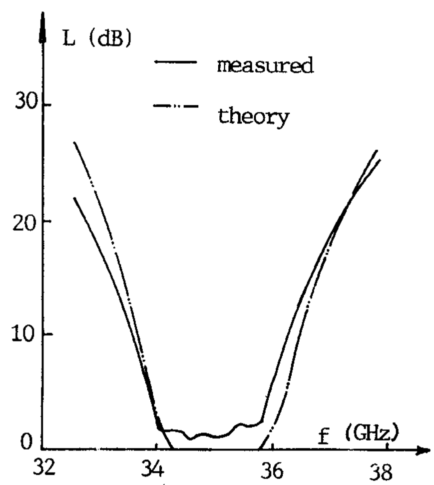

Fig. 9